On the Asymptotic Sum Rate of Downlink Cellular Systems with Random User Locations

Maksym A. Girnyk, Axel Müller, Mikko Vehkaperä, Lars K. Rasmussen, and Mérouane Debbah

***Abstract*—We consider a downlink of a cellular communication system with a multi-antenna base station (BS). A regularized zero forcing (RZF) precoder is employed at the BS to manage the inter-user interference. Using methods from random matrix theory, we derive an asymptotic approximation for the achievable ergodic sum rate, taking into account the randomness from both fading and random user locations. The obtained deterministic approximation describes well the behavior of finite-sized systems and enables computationally efficient optimization of the RZF precoder matrix.**

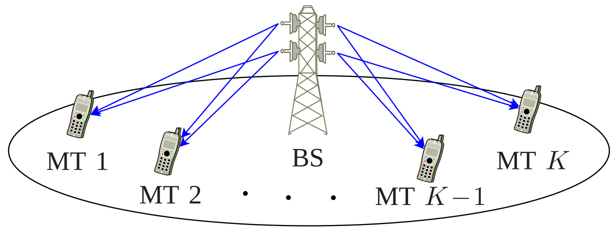

Fig. 1. Downlink cellular communication system.

I. Prelude

Multiple-input multiple-output (MIMO) transmission can significantly increase the performance of a communication system [1] and is therefore seen as a potential building block for future mobile communications. Nowadays, multiple antennas are widely deployed at base stations (BSs) in current cellular systems, which makes MIMO a particularly attractive solution. Multi-user multiple-input single-output (MISO) broadcast setting, where a multi-antenna BS communicates to a set of single-antenna mobile terminals (MTs) through the downlink channel, provides an efficient means to deal with such limiting factors as correlation and line-of-sight components [2]. At the same time, such an approach suffers from inter-user interference. It is the mitigation of the latter that motivates the use of spatial precoding at the BS.

It is known that the sum capacity of Gaussian broadcast vector channels can be achieved by the so-called *dirty-paper coding* (DPC) scheme [3], [4]. This precoding scheme is, however, computationally infeasible in current real-world systems. *Regularized zero forcing* (RZF) precoding serves as a more plausible alternative with close to optimal performance [5]. Due to the particular structure of the corresponding precoder matrix, this scheme turns out to be suitable for analysis using methods from large-dimensional random matrix theory [6]. The setup has been extensively studied in [7], [6, Ch. 14]. The analysis is further generalizable, *e.g.*, to the multi-cell setting [8] and to broadcasting with confidential messages [9].

Usually, the analysis of MIMO channels is done based on the assumption of *deterministic* user placement. This is, however, rarely the case in practice. The MTs are typically freely moving, randomly changing the underlying network topology, which, in turn, influences the performance of the system. To account for *random user locations* in the uplink scenario, [10] proposes to combine the random-matrix analysis with the methods of stochastic geometry [11]. Namely, the positions of the MTs are assumed to be sampled from an independent spatial point process and the corresponding performance metric is averaged over its distribution. The one-dimensional analysis of the uplink multi-user MIMO system performed in [10] is later extended to two- and three-dimensional cell planning in [12] and non-Gaussian channel inputs in [13].

This letter aims at extending the aforementioned analysis to the *downlink scenario*. For that we derive a large-system approximation for the corresponding achievable sum rate, taking into account both the fast fading and the random user locations. The obtained results characterize the system performance under a typical cell configuration. Moreover, the obtained approximation allows the efficient optimization of the RZF precoder matrix at low computational cost. Finally, the results of numerical simulations corroborate our findings.

II. System Configuration

The cellular scenario of interest, depicted in Fig. 1, consists of a BS equipped with M antennas and a set of K mobile terminals (MTs), randomly located within the cell. The latter is described by the cumulative distribution function $F(l)$ of distances between an MT k and the BS (with bounded density $\mathrm{d}F(l)$). The received signal at MT k is of form

$$y_k = \boldsymbol{h}_k^{\mathsf{H}}\boldsymbol{g}_k s_k + \sum_{\substack{j=1\\ j\neq k}}^{K} \boldsymbol{h}_k^{\mathsf{H}}\boldsymbol{g}_j s_j + n_k, \quad (1)$$

where s_k is the symbol dedicated to MT k, $\boldsymbol{g}_k$ is its corresponding precoding vector at the BS, $n_k \sim \mathcal{CN}(0,1)$ is the additive noise and the channel vector between itself and the BS is given by

$$\boldsymbol{h}_k^{\mathsf{H}} = \sqrt{r_k}\,\boldsymbol{w}_k^{\mathsf{H}}\boldsymbol{T}^{1/2}, \quad (2)$$

with r_k being the pathloss (given as a function of distances $r(l) = (1+l)^{-\alpha}$, where α is the pathloss exponent), $\boldsymbol{w}_k$ being a $\mathcal{CN}(\mathbf{0}_M, \frac{\rho}{M}\mathbf{I}_M)$ vector and $0 < \rho < \infty$ being the signal-to-noise ratio (SNR). Here $\boldsymbol{T}$ is a positive semidefinite matrix accounting for the correlation between the antennas at the BS. Note that the correlation matrix is assumed to be independent of the direction from which the signal is observed, meaning, *e.g.*, that a *uniform circular array* [14] is employed at the BS.

The signal-to-interference-plus-noise ratio (SINR) of MT k in the downlink is thus given by

$$\gamma_k = \frac{|\boldsymbol{h}_k^{\mathsf{H}}\boldsymbol{g}_k|^2}{\sum_{\substack{j=1\\ j\neq k}}^{K}|\boldsymbol{h}_k^{\mathsf{H}}\boldsymbol{g}_j|^2+1}. \quad (3)$$

To improve the achievable sum rate in the downlink, a precoder $\boldsymbol{G} = [\boldsymbol{g}_1,\ldots,\boldsymbol{g}_K] \in \mathbb{C}^{M\times K}$ is applied at the BS. In the present letter, we concentrate on RZF precoding at the BS defined by the precoder matrix

$$\boldsymbol{G} = \frac{1}{\sqrt{\Psi}}\left(\boldsymbol{H}^{\mathsf{H}}\boldsymbol{H}+\xi\mathbf{I}_M\right)^{-1}\boldsymbol{H}^{\mathsf{H}}, \quad (4)$$

where $\boldsymbol{H} \triangleq [\boldsymbol{h}_1,\ldots,\boldsymbol{h}_K]^{\mathsf{H}} \in \mathbb{C}^{K\times M}$. The scalar $\xi > 0$ here is a so-called *regularization parameter* [15] which tunes the precoder between conventional *zero forcing* (ZF) and *matched filter* (MF) schemes. Furthermore, the normalization parameter Ψ in (4) is chosen to satisfy the total power constraint $\mathrm{tr}\{\boldsymbol{G}\boldsymbol{G}^{\mathsf{H}}\} \le M$ with equality. That is, for an RZF precoder

$$\Psi \triangleq \frac{1}{M}\mathrm{tr}\left\{\boldsymbol{Z}^2\boldsymbol{H}^{\mathsf{H}}\boldsymbol{H}\right\}, \quad (5)$$

with $\boldsymbol{Z} \triangleq \left(\boldsymbol{H}^{\mathsf{H}}\boldsymbol{H}+\xi\mathbf{I}_M\right)^{-1}$. Note that the BS is assumed to have full channel state information (CSI) of the downlink channel with help of standard training methods [16].

Assuming individual *minimum mean squared error* (MMSE) detection at the MTs and treating the inter-user interference as Gaussian noise, the (normalized) ergodic sum rate is obtained through

$$R_\Sigma(\rho) = \frac{1}{M}\sum_{k=1}^{K}\mathsf{E}_{\boldsymbol{w}_k,r_k}\ln(1+\gamma_k). \quad (6)$$

Unfortunately, this expression requires averaging over the channel coefficients $\boldsymbol{w}_k$ by means of, *e.g.*, Monte Carlo simulations, which does not lead to analytic tractability. In addition to that, one has to perform averaging over the random positions of MTs (random pathloss values r_k) in the cell. Therefore, the main task of the present letter is to find a deterministic equivalent for the above sum rate, which takes care of both aforementioned types of randomness.

III. Asymptotic Sum Rate

In this section, we present an analytically tractable approximation for the sum rate (6), which neither depends on the randomness of the channel, nor on the random positions of the terminals within the cell. The approximation becomes increasingly accurate with an increasing number of antennas at the BS and an increasing number of MTs in the cell. Namely, we define the *large-system limit* (LSL) as the regime where

$$K = \beta M \to \infty \quad (7)$$

with β being a positive finite constant, and having an interpretation of the *system load*. The main result is then summarized in the theorem below.

Theorem 1. *In the LSL, the following holds*

$$R_\Sigma(\rho) - \bar{R}_\Sigma(\rho) \xrightarrow{\text{a.s.}} 0, \quad (8)$$

where the deterministic equivalent, $\bar{R}_\Sigma(\rho)$, is given by

$$\bar{R}_\Sigma(\rho) = \beta\int \ln\left[1+\frac{\rho^2 r^2(l)\chi^2}{\bar{\Upsilon}\rho r(l)+\bar{\Psi}\left(1+\rho r(l)\chi\right)^2}\right]\mathrm{d}F(l), \quad (9)$$

and the corresponding set of parameters is given by

$$\bar{\Psi} = \frac{\psi_1\chi_1}{1-\psi_2\chi_2}, \qquad \bar{\Upsilon} = \frac{\psi_1\chi_2}{1-\psi_2\chi_2}, \quad (10)$$

where further

$$\psi_1 = \beta\int\frac{\rho r(l)\,\mathrm{d}F(l)}{\left(1+\chi\rho r(l)\right)^2}, \quad (11a)$$

$$\psi_2 = \beta\int\frac{\rho^2 r^2(l)\,\mathrm{d}F(l)}{\left(1+\chi\rho r(l)\right)^2}, \quad (11b)$$

$$\chi_1 = \frac{1}{M}\mathrm{tr}\left\{\boldsymbol{T}\left(\psi\boldsymbol{T}+\xi\mathbf{I}_M\right)^{-2}\right\}, \quad (11c)$$

$$\chi_2 = \frac{1}{M}\mathrm{tr}\left\{\boldsymbol{T}^2\left(\psi\boldsymbol{T}+\xi\mathbf{I}_M\right)^{-2}\right\}, \quad (11d)$$

and tuple $\{\psi,\chi\} \in \mathbb{R}^2$ is the unique non-negative solution to the following fixed-point equation

$$\psi = \beta\int\frac{\rho r(l)\,\mathrm{d}F(l)}{1+\chi\rho r(l)}, \quad (12a)$$

$$\chi = \frac{1}{M}\mathrm{tr}\left\{\boldsymbol{T}\left(\psi\boldsymbol{T}+\xi\mathbf{I}_M\right)^{-1}\right\}. \quad (12b)$$

Proof: See Appendix for a sketch of the proof. ■

The above result states that the achievable rate (6) in the LSL converges to its deterministic equivalent (9). The latter requires solving a couple of fixed-point equations and several one-dimensional numerical integration routines in (11a), (11b), and (12a). Meanwhile, it does not involve averaging over the channel realizations, serving as a computationally light approximation for (6).

IV. Optimal Precoder Design

The sum rate of the downlink transmission given in (6), can be optimized by a proper choice of the precoder matrix. The sum rate being an implicit function of the regularization parameter ξ and, hence, the RZF precoder optimization problem

$$\xi^\star = \max_{\xi:\,\xi>0} R_\Sigma(\xi). \quad (13)$$

The difficulty of solving the above problem, apart from its non-convexity, lies in the presence of the expectation operators in the objective function $R_\Sigma(\xi)$ given by (6). This requires numerical averaging with subsequent optimization of ξ, and hence the approach is inefficient. Instead, one can optimize the asymptotic approximation derived in Theorem 1, *i.e.*,

$$\bar{\xi}^\star = \max_{\xi:\,\xi>0} \bar{R}_\Sigma(\xi), \quad (14)$$

which can now be solved using a one-dimensional bisection. The latter has clearly less computational complexity than the direct simulation-based solution of (13), which requires averaging over the channels at each step of the bisection.

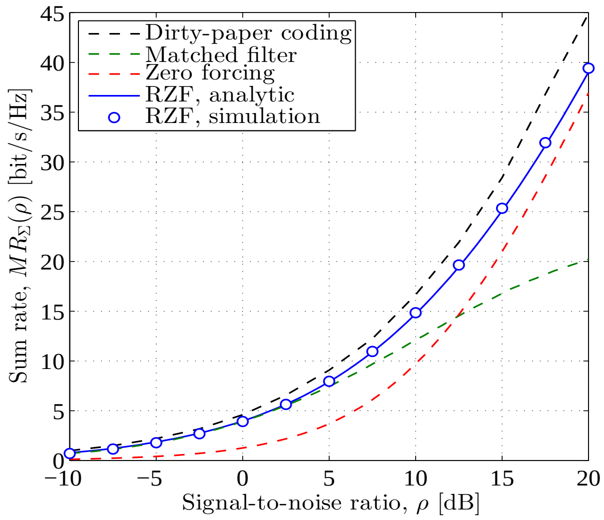

Fig. 2. Achievable sum rate *vs.* SNR for a downlink cellular system with $M = 36$ antennas at the BS and $K = 12$ single-antenna MTs in the uncorrelated scenario. The cell radius and the regularization parameter are set to $D = 2$ and $\xi = 1$, respectively.

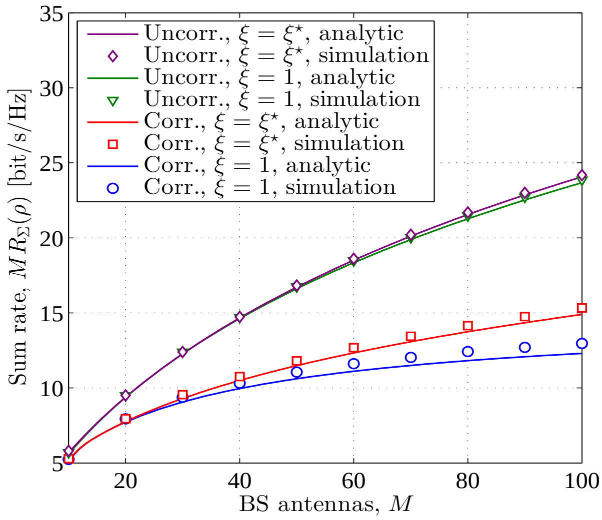

Fig. 3. Achievable sum rate *vs.* number of BS antennas for a downlink cellular system with $K = 10$ single-antenna MTs with RZF precoding. The cell radius and the SNR are set to $D = 2$ and $\rho = 10$ dB, respectively.

V. Simulation Results

Theorem 1 provides a deterministic equivalent for the normalized sum rate of the downlink transmission with RZF precoding, which describes the performance of the system in the LSL. In the finite-sized setting, however, this value, multiplied with the actual (finite) number of antennas, yields an approximation of the actual achievable sum rate. To examine the accuracy of such approximation, we plot in Fig. 2 the sum rate of a cellular communication system, where the corresponding cell has radius $D = 2$, and contains $K = 12$ users, as well as a BS equipped with $M = 36$ antennas. The users are uniformly distributed within the cell. The pathloss is set as $\alpha = 3.7$, and the regularization parameter used by the BS is set to $\xi = 1$. We plot the obtained asymptotic expression (9) as a function of SNR, together with the results of numerical averaging of (6) over 500 channel realizations in the uncorrelated scenario (*i.e.*, i.i.d. $\mathcal{CN}(0, \frac{\rho}{M})$ entries).

In the figure, solid curves denote the analytic results, markers denote the simulated values averaged 500 independent channel realizations. In line with the previous observations, the asymptotic approximation is quite accurate for even for finite antenna numbers (cf. (7)). In addition to the performance of the RZF precoder, we also plot that of MF and ZF alternatives, as well as the performance of DPC obtained following [4]. As expected, it is seen that the RZF precoder always performs better than both MF and ZF, whereas DPC provides an upper bound for its performance. At the same time, expectedly, the performance of RZF at low SNR tends to that of the MF, whilst at high SNR it approaches the performance of the ZF precoder (cf. Fig. 2 in [15]).

In Fig. 3, we study the effects of correlation and optimization of the regularization parameter ξ. To capture the former the antenna array is modeled as a uniform circular array [14]. Hence, the correlation matrix $\boldsymbol{T}$ is generated as

$$\boldsymbol{T} = \boldsymbol{C}\left(\rho_0, \rho_1, \ldots, \rho_{\lceil \frac{M-1}{2} \rceil}, \rho_{\lfloor \frac{M-1}{2} \rfloor}, \ldots, \rho_2, \rho_1\right), \qquad (15)$$

where $\boldsymbol{C}(\cdot)$ is the circulant matrix, $\lceil \cdot \rceil$ and $\lfloor \cdot \rfloor$ are ceiling and floor operators, respectively, while the spatial correlation coefficient ρ_m between an antenna element and its mth neighbor is given by

$$\rho_m = J_0\left(2\pi r_\lambda \sin\frac{m\pi}{M}\right), \qquad (16)$$

with $J_0(\cdot)$ being the first-kind Bessel function of zeroth order and r_λ being the radius of the array (in wavelengths). For the purpose of simulations we set $r_\lambda = 2$. In the figure, we plot the achievable sum rates *vs.* the number of antennas for fixed r_λ. That is, we increase the number of antennas, while limiting the physical size of the array. The SNR is set to $\rho = 10$ dB, and the number of MTs is set to $K = 10$. The rest of the parameters remain unchanged from the setup of Fig. 2.

For the analytic curves optimal regularization parameters, $\xi^{\star}$, have been obtained *via* a one-dimensional bisection method, whereas for the simulation results similar bisection have been performed over the original sum-rate expression (6). From the figure one can observe a gain from optimization of the regularization parameter, which becomes larger in the correlated scenario. Meanwhile, one sees that the accuracy of the large-system approximation worsens in the correlated scenario. Furthermore, quite expectedly, correlation exhibits a negative effect on the system performance.

VI. Conclusions

In this letter, we have derived a deterministic approximation for the achievable ergodic sum rate of downlink cellular communication with a multi-antenna base station. The obtained approximation accounts for both ergodic fading and random locations of the receivers. The results are in good match with the numerical simulations and provide an efficient means for design of the base-station precoder matrix.

APPENDIX

Firstly, we incorporate the RZF precoder into (3) and rewrite the SINR of MT k as follows

$$\gamma_k = \frac{|\boldsymbol{h}_k^{\mathsf{H}}\boldsymbol{Z}\boldsymbol{h}_k|^2}{\boldsymbol{h}_k^{\mathsf{H}}\boldsymbol{Z}\boldsymbol{H}_{\bar{k}}^{\mathsf{H}}\boldsymbol{H}_{\bar{k}}\boldsymbol{Z}\boldsymbol{h}_k+\Psi}, \tag{17}$$

where $\boldsymbol{H}_{\bar{k}} \triangleq [\boldsymbol{h}_1,\ldots,\boldsymbol{h}_{k-1},\boldsymbol{h}_{k+1},\ldots,\boldsymbol{h}_K]^{\mathsf{H}} \in \mathbb{C}^{M\times(K-1)}$.

Next, for *fixed* user positions, proceeding similarly to [6, Ch. 14], we can ultimately show that in the LSL it holds that

- The power normalization term, Ψ, converges to (cf. [6, (14.8), (14.10)])

$$\bar{\Psi} = \frac{\frac{\rho}{M^2}\mathrm{tr}\left\{\boldsymbol{R}\left(\rho\chi\boldsymbol{R}+\mathbf{I}_K\right)^{-2}\right\}\mathrm{tr}\left\{\boldsymbol{T}\left(\psi\boldsymbol{T}+\xi\mathbf{I}_M\right)^{-2}\right\}}{1-\frac{\rho^2}{M^2}\mathrm{tr}\left\{\boldsymbol{R}^2\left(\rho\chi\boldsymbol{R}+\mathbf{I}_K\right)^{-2}\right\}\mathrm{tr}\left\{\boldsymbol{T}^2\left(\psi\boldsymbol{T}+\xi\mathbf{I}_M\right)^{-2}\right\}}, \tag{18}$$

where

$$\psi = \frac{\rho}{M}\mathrm{tr}\left\{\boldsymbol{R}\left(\rho\chi\boldsymbol{R}+\mathbf{I}_K\right)^{-1}\right\}, \tag{19a}$$

$$\chi = \frac{1}{M}\mathrm{tr}\left\{\boldsymbol{T}\left(\psi\boldsymbol{T}+\xi\mathbf{I}_M\right)^{-1}\right\}. \tag{19b}$$

- The received signal power, $S_k \triangleq |\boldsymbol{h}_k^{\mathsf{H}}\boldsymbol{Z}\boldsymbol{h}_k|^2$, converges to (cf. [6, (14.13)])

$$\bar{S}_k = \frac{\rho r_k\chi}{1+\rho r_k\chi}. \tag{20}$$

- The received interference power, $I_k \triangleq \boldsymbol{h}_k^{\mathsf{H}}\boldsymbol{Z}\boldsymbol{H}_{\bar{k}}^{\mathsf{H}}\boldsymbol{H}_{\bar{k}}\boldsymbol{Z}\boldsymbol{h}_k$, converges to (cf. [6, (14.19)])

$$\bar{I}_k = \frac{\rho r_k\bar{\Upsilon}}{1+\rho r_k\chi}, \tag{21}$$

where

$$\bar{\Upsilon} = \frac{\frac{\rho}{M^2}\mathrm{tr}\left\{\boldsymbol{R}\left(\rho\chi\boldsymbol{R}+\mathbf{I}_K\right)^{-2}\right\}\mathrm{tr}\left\{\boldsymbol{T}^2\left(\psi\boldsymbol{T}+\xi\mathbf{I}_M\right)^{-2}\right\}}{1-\frac{\rho^2}{M^2}\mathrm{tr}\left\{\boldsymbol{R}^2\left(\rho\chi\boldsymbol{R}+\mathbf{I}_K\right)^{-2}\right\}\mathrm{tr}\left\{\boldsymbol{T}^2\left(\psi\boldsymbol{T}+\xi\mathbf{I}_M\right)^{-2}\right\}}. \tag{22}$$

At this point, define for convenience the following quantities

$$\psi_1 \triangleq \frac{\rho}{M}\mathrm{tr}\left\{\boldsymbol{R}\left(\rho\chi\boldsymbol{R}+\mathbf{I}_K\right)^{-2}\right\}, \tag{23a}$$

$$\psi_2 \triangleq \frac{\rho^2}{M}\mathrm{tr}\left\{\boldsymbol{R}^2\left(\rho\chi\boldsymbol{R}+\mathbf{I}_K\right)^{-2}\right\}, \tag{23b}$$

$$\chi_1 \triangleq \frac{1}{M}\mathrm{tr}\left\{\boldsymbol{T}\left(\psi\boldsymbol{T}+\xi\mathbf{I}_M\right)^{-2}\right\}, \tag{23c}$$

$$\chi_2 \triangleq \frac{1}{M}\mathrm{tr}\left\{\boldsymbol{T}^2\left(\psi\boldsymbol{T}+\xi\mathbf{I}_M\right)^{-2}\right\}. \tag{23d}$$

In this new notation $\bar{\Psi}$ and $\bar{\Upsilon}$ are given as

$$\bar{\Psi} = \frac{\psi_1\chi_1}{1-\psi_2\chi_2}, \qquad \bar{\Upsilon} = \frac{\psi_1\chi_2}{1-\psi_2\chi_2}, \tag{24}$$

and for the normalized ergodic sum rate we have

$$R_\Sigma(\rho)-\frac{1}{M}\sum_{k=1}^{K}\ln\left[1+\frac{\rho^2 r_k^2\chi^2}{\bar{\Upsilon}\rho r_k+\bar{\Psi}\left(1+\rho r_k\chi\right)^2}\right] \xrightarrow{\text{a.s.}} 0. \tag{25}$$

Let now users distances to the BS be *randomly distributed* over the cell according to distribution $F(l)$. Extending previous results, from the strong law of large numbers one gets

$$\frac{1}{M}\sum_{k}^{K}\frac{\rho r_k}{1+\rho\chi r_k}-\beta\int\frac{\rho r(l)\,\mathrm{d}F(l)}{1+\rho\chi r(l)} \xrightarrow{\text{a.s.}} 0, \tag{26a}$$

$$\frac{1}{M}\sum_{k}^{K}\frac{\rho r_k}{\left(1+\rho\chi r_k\right)^2}-\beta\int\frac{\rho r(l)\,\mathrm{d}F(l)}{\left(1+\rho\chi r(l)\right)^2} \xrightarrow{\text{a.s.}} 0, \tag{26b}$$

$$\frac{1}{M}\sum_{k}^{K}\frac{\rho^2 r_k^2}{\left(1+\rho\chi r_k\right)^2}-\beta\int\frac{\rho^2 r^2(l)\,\mathrm{d}F(l)}{\left(1+\rho\chi r(l)\right)^2} \xrightarrow{\text{a.s.}} 0, \tag{26c}$$

and, additionally, for the normalized sum rate one obtains

$$R_\Sigma(\rho)-\beta\int\ln\left[1+\frac{\rho^2 r^2(l)\chi^2}{\bar{\Upsilon}\rho r(l)+\bar{\Psi}\left(1+\rho r(l)\chi\right)^2}\right]\mathrm{d}F(l) \xrightarrow{\text{a.s.}} 0. \tag{27}$$

REFERENCES

[1] G. Foschini and M. Gans, "On limits of wireless communications in a fading environment when using multiple antennas," *Wireless Pers. Commun.*, vol. 6, no. 3, pp. 311–335, 1998.

[2] D. Gesbert, M. Kountouris, R. W. Heath, C.-B. Chae, and T. Salzer, "Shifting the MIMO paradigm," *IEEE Signal Process. Mag.*, vol. 24, no. 5, pp. 36–46, 2007.

[3] M. H. Costa, "Writing on dirty paper," *IEEE Trans. Inf. Theory*, vol. 29, no. 3, pp. 439–441, 1983.

[4] P. Viswanath and D. N. C. Tse, "Sum capacity of the vector Gaussian broadcast channel and uplink-downlink duality," *IEEE Trans. Inf. Theory*, vol. 49, no. 8, pp. 1912–1921, 2003.

[5] C. B. Peel, B. M. Hochwald, and A. L. Swindlehurst, "A vector-perturbation technique for near-capacity multiantenna multiuser communication-part I: Channel inversion and regularization," *IEEE Trans. Commun.*, vol. 53, no. 1, pp. 195–202, 2005.

[6] R. Couillet and M. Debbah, *Random matrix methods for wireless communications*. Cambridge University Press Cambridge, MA, 2011.

[7] S. Wagner, R. Couillet, M. Debbah, and D. T. Slock, "Large system analysis of linear precoding in correlated MISO broadcast channels under limited feedback," *IEEE Trans. Inf. Theory*, vol. 58, no. 7, pp. 4509–4537, 2012.

[8] J. Zhang, C.-K. Wen, S. Jin, X. Gao, and K.-K. Wong, "Large system analysis of cooperative multi-cell downlink transmission via regularized channel inversion with imperfect CSIT," *IEEE Trans. Wireless Commun.*, vol. 12, no. 10, pp. 4801–4813, 2013.

[9] G. Geraci, R. Couillet, J. Yuan, M. Debbah, and I. B. Collings, "Large system analysis of linear precoding in MISO broadcast channels with confidential messages," *IEEE J. Sel. Areas Commun.*, vol. 31, no. 9, pp. 1660–1671, 2013.

[10] J. Hoydis, A. Müller, R. Couillet, and M. Debbah, "Analysis of multicell cooperation with random user locations via deterministic equivalents," in *Int. Symp. Model. Opt. Mobile, Ad Hoc and Wireless Networks (WiOpt)*, 2012, pp. 374–379.

[11] M. Haenggi, *Stochastic geometry for wireless networks*. Cambridge University Press, 2012.

[12] A. Müller, J. Hoydis, R. Couillet, and M. Debbah, "Optimal 3D cell planning: A random matrix approach," in *Proc. IEEE Global Commun. Conf. (GLOBECOM)*, 2012, pp. 4512–4517.

[13] M. A. Girnyk, M. Vehkapera, and L. K. Rasmussen, "Multi-cell cooperation with random user locations under arbitrary signaling," in *Proc. IEEE Inf. Theory Workshop (ITW)*, 2013, pp. 574–578.

[14] T. S. Pollock, T. D. Abhayapala, and R. A. Kennedy, "Antenna saturation effects on MIMO capacity," in *Proc. IEEE Int. Conf. Commun. (ICC)*, vol. 4, 2003, pp. 2301–2305.

[15] E. Björnson, M. Bengtsson, and B. Ottersten, "Optimal multiuser transmit beamforming: A difficult problem with a simple solution structure," *IEEE Signal Process. Mag.*, vol. 31, no. 4, pp. 142–148, 2014.

[16] M. Biguesh and A. B. Gershman, "Training-based MIMO channel estimation: A study of estimator tradeoffs and optimal training signals," *IEEE Trans. Signal Process.*, vol. 54, no. 3, pp. 884–893, 2006.